Journal of Nuclear Medicine, published on May 15, 2020 as doi:10.2967/jnumed.120.243139

^{124}I-MIBG PET-CT to monitor metastatic disease in children with relapsed neuroblastoma

Mariam S. Aboian[1,2], Shih-ying Huang[1], Miguel Hernandez-Pampaloni[1], Randall A. Hawkins[1,†], Henry F. VanBrocklin[1], Yoonsuk Huh[1], Kieuhoa T. Vo[3], W. Clay Gustafson[3], Katherine K. Matthay[3], and Youngho Seo[1,4]

[1]Department of Radiology and Biomedical Imaging, University of California, San Francisco, San Francisco, CA

[2]Department of Radiology and Biomedical Imaging, Yale University, New Haven, CT

[3]Department of Pediatrics, University of California, San Francisco, San Francisco, CA

[4]Department of Radiation Oncology, University of California, San Francisco, San Francisco, CA

[†]Deceased

***Corresponding author:**

Youngho Seo, Ph.D

Professor

UCSF Physics Research Laboratory

Department of Radiology and Biomedical Imaging

University of California, San Francisco, CA 94143-0946

Phone: 415-353-9464; E-mail: youngho.seo@ucsf.edu

Short Running Title: ^{124}I-MIBG to monitor MIBG therapy

Abstract

The metaiodobenzylguanidine (MIBG) scan is one of the most sensitive noninvasive lesion detection modalities for neuroblastoma. Unlike ^{123}I-MIBG, ^{124}I-MIBG allows high-resolution positron emission tomography (PET). We evaluated ^{124}I-MIBG PET/CT for its diagnostic performance directly compared to paired ^{123}I-MIBG scans.

Methods: Prior to ^{131}I-MIBG therapy, standard ^{123}I-MIBG scans (5.2 MBq/kg) that include whole-body (anterior-posterior) planar scans and focused field of view (FOV) single photon emission computed tomography combined with CT (SPECT/CT) as well as whole-body ^{124}I-MIBG PET/CT (1.05 MBq/kg) were performed in 7 patients. After therapy, 2 of 7 patients also completed ^{124}I-MIBG PET/CT as well as paired ^{123}I-MIBG planar and SPECT/CT scans. One patient received ^{124}I-MIBG PET/CT only after therapy. We evaluated all 8 patients who showed at least one ^{123}I-MIBG-positive lesion with a total of 10 scans. In 8 pairs, ^{123}I-MIBG and ^{124}I-MIBG were performed within 1 month of each other. Locations of identified lesions, the number of total lesions, and the Curie scores were recorded for ^{123}I-MIBG and ^{124}I-MIBG scans. Finally, for five patients who completed at least three PET/CT scans after administration of ^{124}I-MIBG, we estimated the effective dose of ^{124}I-MIBG.

Results: ^{123}I-MIBG whole-body planar scans, focused FOV SPECT/CT scans, and whole-body ^{124}I-MIBG PET scans found 25, 32, and 87 total lesions respectively. There was a statistically significant difference in detecting lesions on ^{124}I-MIBG PET/CT as compared to ^{123}I-MIBG planar scans ($P < 0.0001$) and ^{123}I-MIBG SPECT/CT ($P < 0.0001$). The Curie scores were also higher for ^{124}I-MIBG PET/CT as compared to those for ^{123}I-MIBG planar and SPECT/CT in 6 out of 10 scans. ^{124}I-MIBG PET/CT demonstrated better detection of lesions throughout the body including chest, spine, head and neck, and extremities. The effective dose estimated for patient-

specific ^{124}I-MIBG was approximately ten times that of ^{123}I-MIBG; however, given that we administered a very low activity of ^{124}I-MIBG (1.05 MBq/kg), the effective dose was only approximately twice that of ^{123}I-MIBG despite the large difference in half-lives (100 vs. 13.2 hours).

Conclusion: The first in human use of low-dose ^{124}I-MIBG PET for monitoring disease burden demonstrated superior tumor detection capability as compared to ^{123}I-MIBG planar and SPECT/CT scans.

Keywords: neuroblastoma, ^{124}I, ^{124}I-MIBG, metaiodobenzylguanidine, PET/CT

INTRODUCTION

Neuroblastoma is the most common cancer in children less than 1 year old and accounts for approximately 6-8% of all cancers in children *(1)*. Approximately 90% of neuroblastoma cases are diagnosed before the age of 5 years. Neuroblastoma develops along the sympathetic nervous system with approximately 80% of the tumors occurring in the abdomen *(2)*. Metastatic disease is found in about half the cases at the time of diagnosis, with most frequent sites of metastatic disease being bone and bone marrow, involving osseous structures from the skull and spine to appendicular skeleton, followed by liver, and skin *(3)*. There are several factors that are involved in staging and risk classification of neuroblastoma, defined by the recent International Neuroblastoma Risk Group system (INRG) *(4)*. Initial assessment of tumor extent uses the INRG staging of L1 (localized tumor without image-defined risk factors for surgery), L2 (locoregional tumor with image-defined risk factors), and M (metastatic) or MS (metastatic in infant <18 months with metastases limited to liver, skin and bone marrow) *(5)*. Other clinical an biologic risk factors include age, MYCN gene status, tumor cell histology and ploidy. Based on INRG staging system (INRGSS), ^{123}I-metaiodobenzylguanidine (MIBG) planar scintigraphy is recommended prior to tumor excision during diagnosis of neuroblastoma and during follow-up after treatment for monitoring extent of tumor and response to therapy *(3,6)*. Previous studies showed that ^{123}I-single photon emission computed tomography combined with CT (SPECT/CT) imaging provides better assessment of metastatic disease as compared to planar ^{123}I-MIBG imaging due to improved anatomical localization and improved lesion contrast in SPECT/CT versus planar imaging *(7,8)*.

Iodine-124 is a positron-emitting radionuclide that has 4.2 day half-life, making it attractive for delayed clinical imaging and dosimetry. ^{124}I-MIBG PET has been used for imaging of malignant pheochromocytoma demonstrating improved tumor delineation due to higher resolution images as compared to ^{123}I-MIBG SPECT *(9)*. We have previously shown that ^{124}I-MIBG PET/CT can be used in children with neuroblastoma for accurate tumor dosimetry before ^{131}I-MIBG therapy *(10,11)*.

In our study, we performed PET/CT imaging studies using no-carrier-added ^{124}I-MIBG in all patients, which is particularly important since it is a direct match to a recently approved no-carrier-added ^{131}I-MIBG (Azedra®, Progenics Pharmaceuticals). Here, we report the results of first-in-human imaging studies with no-carrier-added ^{124}I-MIBG PET/CT in patients with neuroblastoma.

MATERIALS AND METHODS

Subjects

Patients were eligible who had relapsed or refractory high-risk neuroblastoma, with confirmation of the diagnosis by histologic verification of the tumor, or by typical infiltration of tumor cells in bone marrow with elevated urinary catecholamines. They also had age greater than or equal to three years, and had consented to ^{131}I-MIBG treatment. Patients who required general anesthesia for MIBG imaging studies were excluded. The study was approved by our institutional review board and informed consent was obtained from all subjects and/or guardians.

Imaging

No-carrier added ^{124}I-MIBG was either synthesized using resins provided by our industry collaborator (Progenics Pharmaceuticals, New York, NY) at our institution, or purchased from a commercial radiopharmacy (3D Imaging, Little Rock, AR) under IND#113907. No difficulties were encountered in the supply of ^{124}I MIBG and in quality assurance steps during our study. ^{124}I-MIBG PET/CT scans were obtained on a Discovery VCT PET/CT camera (GE Healthcare) for 6 patients and a Gemini TF PET/CT camera (Philips Healthcare) for 2 patients. There were no significant differences that could impact clinical interpretation between the PET scans performed on either the Discovery VCT or Gemini TF. This imaging study was performed in parallel with a pretherapy dosimetry study for 5 patients; therefore these 5 patients imaged prior to MIBG therapy had multiple imaging timepoints with 24 hr scan being used for image interpretation, while post therapy scan was a single scan at 24 hours after ^{124}I-MIBG administration. For those who did not complete multiple time points for the pretherapy dosimetry study, as for the post therapy scan, only 24 hour imaging time point was captured after ^{124}I-MIBG administration. Because of the low activity of ^{124}I-MIBG administered, PET data were acquired for at least 4 minutes per bed position. ^{123}I-MIBG scan using whole body planar imaging as well as focused field of view (FOV) SPECT/CT was performed on all patients 24 hours after 5.2 MBq/kg of the radiotracer administered. The studies were performed between 2013 and 2017. Lesion locations, total number of lesions, and Curie scores *(3)* were recorded using two independent interpretations by two nuclear medicine physicians (MHP, RH). Curie score was calculated per standard method as described below for ^{123}I-MIBG and ^{131}I-MIBG planar scans. For ^{124}I-MIBG PET, the Curie score was calculated using the MIP images. Planar, SPECT, and PET/CT scans that were compared in terms of lesion number and Curie score were performed within 1 month of each other. All positive lesions were confirmed on cross-sectional

imaging. The scoring was performed based on division of the body into nine anatomic sectors for osseous lesions (skull, upper arms, lower arms, chest, upper spine, lower spine, pelvis, upper legs, and lower legs) and a separate section for any extraosseous metastases as described in Matthay et al. *(12)*. In each of the regions, the lesions were scored as 0 for no lesion within the segment, 1 for one lesion within the segment, 2 for more than one lesion per segment, and 3 for greater than 50% involvement of the segment. The absolute score was obtained by adding the scores of all the segments. There was a high concordance rate between the two reads with Fleiss' kappa measuring 0.783 (CI: 0.6417, 0.9702). Upon discrepancy between the readers, the higher value was used for the study.

Radiation dosimetry of ^{124}I-MIBG

For the five patients who completed ^{124}I-MIBG dosimetry scans, we performed full dose estimation, particularly for effective dose. For the dosimetry of ^{124}I-MIBG, PET imaging was performed within the first 4 hours after injection, 24 hr, 48 hr, and 120 hr after administration of ^{124}I-MIBG. The general method for our dose calculation was described previously *(10)*. For the current study, one improved technique, using patient-specific CT as a voxelized phantom for Monte Carlo simulation, over what was reported before. From organ doses calculated from the Monte Carlo simulation combined with time-integrated activity coefficients (TIACs), also known as residence times, derived from 3 or 4 PET/CT images, ICRP103 weighting factors were applied, and effective doses for each patient were calculated.

Statistical analysis

Continuous variable data were analyzed across pretreatment and posttreatment scans using two samples *t*-tests. Categorical variable data were analyzed with chi-squared test. Statistical analysis was performed on STATA (StataCorp, College Station, Texas).

RESULTS

In our study, 5 of the enrolled patients also underwent ^{131}I-MIBG therapy for widely metastatic neuroblastoma and 8 total patients underwent the paired imaging with standard whole body planar and focused FOV SPECT/CT ^{123}I-MIBG. In the five patients who received therapy, pretherapy whole body ^{124}I-MIBG PET/CT was performed and in two patients both pretherapy and follow up posttherapy ^{124}I-MIBG PET/CT were performed. The mean age of the patients we evaluated was 11.6 with the range of 6 – 23.

Detection of lesions using ^{124}I-MIBG PET/CT versus ^{123}I-MIBG scans

^{123}I-MIBG whole-body planar scans, focused FOV SPECT/CT scans, and whole-body ^{124}I-MIBG PET scans found 25, 32, and 87 lesions respectively in 10 sets of matched scan data (Figure 1). All but one (i.e., 24) lesion detected by ^{123}I-MIBG planar scans were clearly detected on ^{124}I-MIBG PET/CT. The single lesion that was not detected by ^{124}I-MIBG PET/CT but detected by ^{123}I-MIBG planar scan was located in the thoracic spine. Evaluation of ^{124}I-MIBG uptake within the thoracic spine for this patient was limited due to significant motion of the patient during that section of the scan and background uptake, which affected detection of this lesion. However, 62 lesions that were detected on ^{124}I-MIBG PET/CT were not detected by ^{123}I-MIBG planar scans and 55 lesions not detected by ^{123}I-MIBG SPECT/CT (Figure 1A). The

difference in detection of individual lesions on ^{124}I-MIBG PET/CT was statistically significant as compared to ^{123}I-MIBG planar scans ($P < 0.0001$) and ^{123}I-MIBG SPECT/CT ($P < 0.0001$).

Higher lesion detection by ^{124}I-MIBG PET results in higher Curie scores

Ten ^{124}I-MIBG PET scans that were performed within 2 weeks of ^{123}I-MIBG planar imaging scans. Curie scores were obtained by blinded review by two nuclear medicine physicians with expertise in pediatric imaging. Out of 10 scans, 6 had higher Curie scores on ^{124}I-MIBG PET/CT as compared to ^{123}I-MIBG planar imaging scans and 4 had higher Curie scores than ^{123}I-MIBG planar and SPECT/CT combined interpretation (Figure 1B).

Localization of lesions based on the part of the body

Cross-sectional imaging provides an advantage in localizing lesions with complex 3D structures. In our patient cohort, ^{124}I-MIBG PET/CT was more sensitive in detecting lesions within the chest with the chest component of the Curie score being higher in 4 patients as compared to planar imaging and in 3 patients as compared to SPECT/CT. In head and neck region, two patients had higher head components of the Curie scores as compared to planar imaging and one patient had higher scores as compared to SPECT/CT (Figure 2 and Supplemental Tables 1-8). Another region of high discrepancy between the planar imaging read and the PET/CT were thoracic and lumbar spine. In thoracic spine, there were four patients with higher component score on PET/CT as compared to ^{123}I planar imaging and two patients as compared to SPECT/CT. These results suggest, that ^{124}I-MIBG PET/CT is better at detecting lesions within chest, spine, and head and neck regions than SPECT/CT, which are traditionally evaluated with SPECT/CT for more accurate lesion detection than planar imaging.

Radiation exposure from low-dose ^{124}I-MIBG PET/CT compared to ^{123}I-MIBG planar imaging and SPECT/CT

There is a significant difference in half-lives between ^{124}I and ^{123}I, with the former being 100 hours and the latter being 13.2 hours. This potentially can result in higher effective dose for patients undergoing ^{124}I-MIBG. In our study, the estimated effective doses were, 0.161 mSv/MBq for 122-kg female, 0.235 mSv/MBq for 63-kg male, 0.339 mSv/MBq for 40-kg male, 0.706 mSv/MBq for 29-kg female, and 0.795 mSv/MBq for 23-kg female patients. These effective dose values were in a good agreement with our estimated effective doses for human subjects extrapolated from the data obtained in murine models *(13)*, The previously estimated effective doses, using ICRP103 weighting factors, were 0.252 mSv/MBq for 73.7-kg male, 0.342 mSv/MBq for 57-kg female, 0.388 mSv/MBq for 56.8-kg 15-year old, 0.578 mSv/MBq for 33.2-kg 10-year old, 1.027 mSv/MBq for 19.8-kg 5-year old. These values are approximately 10 times higher than those of ^{123}I-MIBG (0.019 mSv/MBq for 73.7-kg male). However, the effective dose for ^{124}I-MIBG scan (1.05 MBq/kg administered) was only approximately twice the dose for ^{123}I-MIBG scan (5.2 MBq/kg administered) because of the low administered dose protocol.

DISCUSSION

Accurate detection of metastatic disease is critical in high-risk neuroblastoma because semiquantitative MIBG scoring has been shown to correlate with patient outcomes at diagnosis *(12)* and during treatment *(14,15)*. Curie score has been developed for planar ^{123}I-MIBG scans for detection and quantitation of metastatic disease *(16)*, but may be prone to interpretation bias

when there is faint uptake or difficulty in identification of disease within anatomically complex regions of head and neck, spine, chest, and pelvis. To circumvent this limitation, many institutions perform limited SPECT/CT of abdomen and pelvis to improve detection of disease with modification of the Curie score to reflect findings on planar and SPECT/CT images. Whole body SPECT/CT is not routinely performed in clinical practice due to the length of exam, which can take up to more than an hour. On the other hand, whole body PET/CT can be performed within 40 minutes even with a low-dose protocol similar to that utilized in our study, and can provide a single unified semiquantitative score for patient metastatic status.

To the best of our knowledge, our study is first-in-human imaging of metastatic neuroblastoma with ^{124}I-MIBG PET/CT. We demonstrated that there is superior tumor detection capability by ^{124}I-MIBG PET/CT as compared to those of ^{123}I-MIBG planar and SPECT/CT imaging. The increased detection of tumors also translated to higher Curie scores in patients as interpreted by two board-certified nuclear medicine physicians. The lesions that were better detected on ^{124}I-MIBG PET were predominantly within the chest, spine, head and neck region, and upper and lower extremities. The long half-life of the ^{124}I-MIBG allowed subsequent imaging of patients over the course of 3 days, thus allowing quantitative assessment of ^{124}I-MIBG dynamic binding and allows better prediction of dosimetry in addition to diagnostic quality imaging. Effective dose to the patients in our study was only twice of the ^{123}I-MIBG scan; therefore this tracer could be considered a safe alternative for patients with metastatic neuroblastoma.

One limitation of our study was the small number of patients, which may have been due to the fact that most children with neuroblastoma are young and would require anesthesia for these additional studies. We had 10 ^{124}I-MIBG PET scans performed on 8 patients during

different time points of their treatment with ^{131}I-MIBG therapy, with the majority imaged prior to treatment. Because few patients consented to the follow up ^{124}I-MIBG PET/CT scan, information is lacking on evaluation of response and correlation with progression-free survival. Now that we have established the much greater sensitivity for detection of metastatic disease than the standard ^{123}I-MIBG, further research on this radiotracer in a larger number of patients is indicated, without the need for concomitant ^{123}I-MIBG scans. Also, for patients who received both serial ^{124}I-MIBG scans and ^{131}I-MIBG therapies, we did not have serial ^{131}I-MIBG scan data to calculate the absorbed dose from ^{131}I-MIBG therapy and to compare ^{131}I-MIBG doses with predicted doses from ^{124}I-MIBG scans. Although we had limited data to compare predicted lesion doses with therapy response for these patients, the number of patients is too small to claim any statistical significance at this point. Further research into detection of neuroblastoma with low uptake of MIBG-based tracers (i.e., ^{123}I-MIBG and ^{124}I-MIBG) and comparison to ^{18}F-fluorodeoxyglucose (FDG) PET will also be needed to establish the role of ^{124}I-MIBG PET will play in clinical management of patients. This will establish the role of improved detection of metastatic disease in diagnosis and monitoring of metastatic neuroblastoma. Effective dose calculated for ^{124}I-MIBG in our cohort was in the range of 0.161 – 0.795 mSv/MBq, as we showed all calculated values for each individual we evaluated in the Results section above, which is approximately 10-20 times of the effective dose of FDG in the pediatric population *(17)*. For this reason, we chose to inject a very low amount of activity (1.05 MBq/kg) with the trade-off of scanning longer time and noisy images overall. Hence, we propose that ^{124}I-MIBG PET/CT may play an important role in follow up imaging of patients and further investigation into negative predictive value of this test for patient outcomes is under way.

DISCLOSURE

This work was supported in part by the National Cancer Institute under grant R01 CA154561 and P01 CA81403, and by the Alex Scott Lemonade and Dougherty Foundations.

Authors' Conflict of interest

No conflict of interest.

ACKNOWLEDGMENTS

The authors would like to thank the clinical coordinators, the cyclotron team, technologists, nurses, and physicians who made this study possible at UCSF. We also appreciate Progenics Pharmaceuticals for their sharing the resins for ^{124}I-MIBG for our initial human studies. We are particularly grateful to the late Dr. Randall Hawkins and Xiao Wu who made significant contributions to the present study.

KEY POINTS

QUESTION: Is low-dose no-carrier-added ^{124}I-MIBG PET/CT superior to 123I-MIBG planar and SPECT/CT imaging for monitoring disease burden in patients with relapsed neuroblastoma?

PERTINENT FINDINGS: At a low effective dose (~2 times of that of ^{123}I-MIBG), ^{124}I-MIBG PET/CT scans showed a statistically significant superior detection of lesions when compared to ^{123}I-MIBG planar and SPECT/CT scans. The Curie scores were also shown to be higher with ^{124}I-MIBG PET/CT in 6 out of 10 scans evaluated in the stuy.

IMPLICATIONS FOR PATIENT CARE: ^{124}I-MIBG PET/CT may replace currently performed ^{123}I-MIBG planar and SPECT/CT in monitoring disease burden in patients with replased neuroblastoma.

REFERENCES

1. Berthold F, Spix C, Kaatsch P, Lampert F. Incidence, Survival, and Treatment of Localized and Metastatic Neuroblastoma in Germany 1979-2015. *Paediatr Drugs*. 2017;19:577-593.
2. Brisse HJ, McCarville MB, Granata C, et al. Guidelines for imaging and staging of neuroblastic tumors: consensus report from the International Neuroblastoma Risk Group Project. *Radiology*. 2011;261:243-257.
3. Bar-Sever Z, Biassoni L, Shulkin B, et al. Guidelines on nuclear medicine imaging in neuroblastoma. *Eur J Nucl Med Mol Imaging*. 2018;45:2009-2024.
4. Parikh NS, Howard SC, Chantada G, et al. SIOP-PODC adapted risk stratification and treatment guidelines: Recommendations for neuroblastoma in low- and middle-income settings. *Pediatr Blood Cancer*. 2015;62:1305-1316.
5. Matthay KK, Shulkin B, Ladenstein R, Michon J, Giammarile F, Lewington V, Pearson AD, Cohn SL. Criteria for evaluation of disease extent by (123)I-metaiodobenzylguanidine scans in neuroblastoma: a report for the International Neuroblastoma Risk Group (INRG) Task Force. *Br J Cancer*. 2010;102:1319-1326.
6. Uehara S, Yoneda A, Oue T, et al. Role of surgery in delayed local treatment for INSS 4 neuroblastoma. *Pediatr Int*. 2017;59:986-990.
7. Rozovsky K, Koplewitz BZ, Krausz Y, Revel-Vilk S, Weintraub M, Chisin R, Klein M. Added value of SPECT/CT for correlation of MIBG scintigraphy and diagnostic CT in neuroblastoma and pheochromocytoma. *AJR Am J Roentgenol*. 2008;190:1085-1090.
8. Rufini V, Fisher GA, Shulkin BL, Sisson JC, Shapiro B. Iodine-123-MIBG imaging of neuroblastoma: utility of SPECT and delayed imaging. *J Nucl Med*. 1996;37:1464-1468.
9. Hartung-Knemeyer V, Rosenbaum-Krumme S, Buchbender C, et al. Malignant pheochromocytoma imaging with [124I]mIBG PET/MR. *J Clin Endocrinol Metab*. 2012;97:3833-3834.
10. Huang SY, Bolch WE, Lee C, et al. Patient-specific dosimetry using pretherapy [(1)(2)(4)I]m-iodobenzylguanidine ([(1)(2)(4)I]mIBG) dynamic PET/CT imaging before [(1)(3)(1)I]mIBG targeted radionuclide therapy for neuroblastoma. *Mol Imaging Biol*. 2015;17:284-294.
11. Seo Y, Gustafson WC, Dannoon SF, et al. Tumor dosimetry using [124I]m-iodobenzylguanidine microPET/CT for [131I]m-iodobenzylguanidine treatment of neuroblastoma in a murine xenograft model. *Mol Imaging Biol*. 2012;14:735-742.
12. Matthay KK, Edeline V, Lumbroso J, et al. Correlation of early metastatic response by 123I-metaiodobenzylguanidine scintigraphy with overall response and event-free survival in stage IV neuroblastoma. *J Clin Oncol*. 2003;21:2486-2491.
13. Lee CL, Wahnishe H, Sayre GA, et al. Radiation dose estimation using preclinical imaging with 124I-metaiodobenzylguanidine (MIBG) PET. *Med Phys*. 2010;37:4861-4867.
14. Kushner BH, Yeh SD, Kramer K, Larson SM, Cheung NK. Impact of metaiodobenzylguanidine scintigraphy on assessing response of high-risk neuroblastoma to dose-intensive induction chemotherapy. *J Clin Oncol*. 2003;21:1082-1086.
15. Yanik GA, Parisi MT, Naranjo A, et al. Validation of Postinduction Curie Scores in High-Risk Neuroblastoma: A Children's Oncology Group and SIOPEN Group Report on SIOPEN/HR-NBL1. *J Nucl Med*. 2018;59:502-508.

16. Sharp SE, Trout AT, Weiss BD, Gelfand MJ. MIBG in Neuroblastoma Diagnostic Imaging and Therapy. *Radiographics*. 2016;36:258-278.
17. Quinn BM, Gao Y, Mahmood U, Pandit-Taskar N, Behr G, Zanzonico P, Dauer LT. Patient-adapted organ absorbed dose and effective dose estimates in pediatric 18F-FDG positron emission tomography/computed tomography studies. *BMC Med Imaging*. 2020;20:9.

Figures

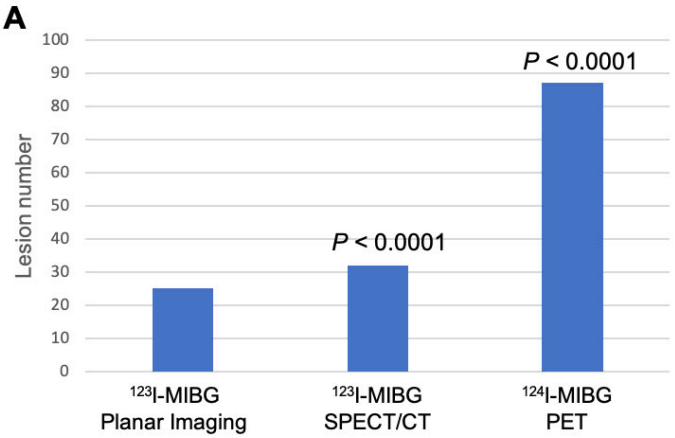

B

scan #	Pre or post therapy		
	I-123 MIBG Planar imaging	I-123 MIBG SPECT imaging	I-124 MIBG PET
1	4	*	9
2	*	*	0
3	18	*	20
4	20	20	20
5	2	6	8
6	2	2	3
7	2	2	6
8	1	1	1
9	9	9	18
10	14	14	14

Figure 1: ^{124}I-MIBG PET/CT detects more lesions than ^{123}I-MIBG planar imaging, ^{123}I-MIBG SPECT/CT and results in higher Curie Scores. (A) The number of lesions were quantified on ^{123}I-MIBG planar and SPECT/CT scans and compared to number of lesions identified on ^{124}I-MIBG PET scans among all 8 patients. There is a statistically significant difference in the amount of lesions detected on ^{124}I-MIBG PET scan as compared to ^{123}I-MIBG planar or SPECT/CT imaging. (B) Curie score comparison between ^{123}I-MIBG planar scan, SPECT/CT, and ^{124}I-MIBG PET scans demonstrates higher overall curies scores on PET imaging. The Curie score was determined by two nuclear medicine physicians for each scan and there were higher Curie scores on ^{124}I-MIBG PET scan for 6 scans as compared to planar and SPECT/CT ^{123}I-MIBG.

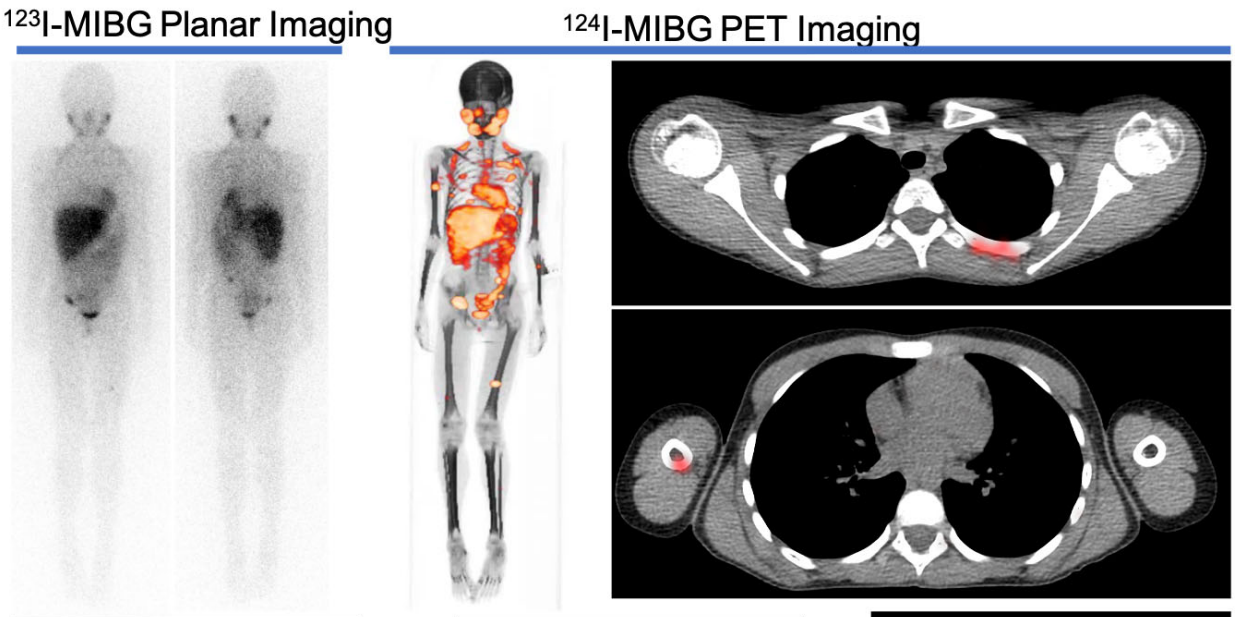

Region	Score (reader 1)	Score (reader 2)
Head	1	1
Chest	0	0
T-spine	0	0
L-spine	0	0
Pelvis	2	2
Upper arms	0	0
Lower arms	0	0
Femurs	1	1
Lower legs	0	0
Soft tissue	0	0
Total score	4	4

Region	Score (reader 1)	Score (reader 2)
Head	2	1
Chest	2	2
T-spine	0	0
L-spine	0	0
Pelvis	2	2
Upper arms	1	1
Lower arms	0	0
Femurs	2	2
Lower legs	0	0
Soft tissue	0	0
Total score	9	8

Figure 2: Regional Curie score components are better evaluated on ^{124}I-MIBG PET as compared to ^{123}I-MIBG planar and SPECT CT. ^{123}I-MIBG planar imaging of same patient is compared to ^{124}I-MIBG PET imaging. Planar anterior and posterior views are included. ^{124}I-MIBG PET 3D volume rendering and cross-sectional superimposed images are demonstrated to the right. Better detection of lesions was predominantly noted within the chest, extremities, spine, and head and neck regions. In this patient, lesions within the chest, upper arms, and head were better detected on ^{124}I-MIBG PET.

Supplemental Tables 1-8: Curie score measurements in individual patients in pre-therapy and post-therapy imaging with description of the score by anatomical location. Individual patients are represented in 1-8.

1	Pre-Therapy Curie Score			Post-Therapy Curie Score		
	I-123 MIBG Planar imaging	I-123 MIBG SPECT imaging	I-124 MIBG PET	I-123 MIBG Planar imaging	I-123 MIBG SPECT imaging	I-124 MIBG PET
Head	1		2			0
Chest	0		2			0
T spine	0		0			0
L spine	0		0			0
Pelvis	2		2			0
Upper Arms	0		1			0
Lower Arms	0		0			0
Femurs	1		2			0
Lower Legs	0		0			0
Soft tissue	0		0			0
Total score	4		9			0

2	Pre-Therapy Curie Score			Post-Therapy Curie Score		
	I-123 MIBG Planar imaging	I-123 MIBG SPECT imaging	I-124 MIBG PET	I-123 MIBG Planar imaging	I-123 MIBG SPECT imaging	I-124 MIBG PET
Head	2		2	2	2	2
Chest	2		2	2	2	2
T spine	2		3	3	3	3
L spine	2		3	3	3	3
Pelvis	2		2	2	2	2
Upper Arms	3		3	3	3	3
Lower Arms	0		0	0	0	0
Femurs	3		3	3	3	3
Lower Legs	2		2	2	2	2
Soft tissue	0		0	0	0	0
Total score	18		20	20	20	20

3	Pre-Therapy Curie Score			Post-Therapy Curie Score		
	I-123 MIBG Planar imaging	I-123 MIBG SPECT imaging	I-124 MIBG PET	I-123 MIBG Planar imaging	I-123 MIBG SPECT imaging	I-124 MIBG PET
Head	0			0	0	0
Chest	0			0	1	1
T spine	0			0	1	1
L spine	0			0	2	2
Pelvis	2			2	2	2
Upper Arms	0			0	0	0
Lower Arms	0			0	0	0
Femurs	0			0	0	2
Lower Legs	0			0	0	0
Soft tissue	0			0	0	0
Total score	2			2	6	8

4	Pre-Therapy Curie Score			Post-Therapy Curie Score		
	I-123 MIBG Planar imaging	I-123 MIBG SPECT imaging	I-124 MIBG PET	I-123 MIBG Planar imaging	I-123 MIBG SPECT imaging	I-124 MIBG PET
Head	0	0	0	0		
Chest	0	0	1	0		
T spine	0	0	0	0		
L spine	0	0	0	0		
Pelvis	0	0	0	0		
Upper Arms	0	0	0	0		
Lower Arms	0	0	0	0		
Femurs	0	0	0	0		
Lower Legs	0	0	0	0		
Soft tissue	2	2	2	0		
Total score	2	2	3	0		

5	Pre-Therapy Curie Score			Post-Therapy Curie Score		
	I-123 MIBG Planar imaging	I-123 MIBG SPECT imaging	I-124 MIBG PET	I-123 MIBG Planar imaging	I-123 MIBG SPECT imaging	I-124 MIBG PET
Head	2	2	1	0	0	
Chest	0	0	2	0	0	
T spine	0	0	1	0	0	
L spine	0	0	0	0	0	
Pelvis	0	0	0	0	0	
Upper Arms	0	0	0	0	0	
Lower Arms	0	0	0	0	0	
Femurs	0	0	1	1	1	
Lower Legs	0	0	1	0	0	
Soft tissue	0	0	0	0	0	
Total score	2	2	6	1	1	

6	Pre-Therapy Curie Score			Post-Therapy Curie Score		
	I-123 MIBG Planar imaging	I-123 MIBG SPECT imaging	I-124 MIBG PET	I-123 MIBG Planar imaging	I-123 MIBG SPECT imaging	I-124 MIBG PET
Head	0	0	0			
Chest	0	0	0			
T spine	0	0	0			
L spine	0	0	0			
Pelvis	0	0	0			
Upper Arms	0	0	0			
Lower Arms	0	0	0			
Femurs	1	1	1			
Lower Legs	0	0	0			
Soft tissue	0	0	0			
Total score	1	1	**1**			

7	Pre-Therapy Curie Score			Post-Therapy Curie Score		
	I-123 MIBG Planar imaging	I-123 MIBG SPECT imaging	I-124 MIBG PET	I-123 MIBG Planar imaging	I-123 MIBG SPECT imaging	I-124 MIBG PET
Head	1	1	2			
Chest	1	1	2			
T spine	0	0	2			
L spine	2	2	2			
Pelvis	2	2	2			
Upper Arms	0	0	2			
Lower Arms	0	0	2			
Femurs	2	2	2			
Lower Legs	1	1	2			
Soft tissue	0	0	0			
Total score	9	9	18			

8	Pre-Therapy Curie Score			Post-Therapy Curie Score		
Pt 1010	I-123 MIBG Planar imaging	I-123 MIBG SPECT imaging	I-124 MIBG PET	I-123 MIBG Planar imaging	I-123 MIBG SPECT imaging	I-124 MIBG PET
Head	2	2	2			
Chest	2	2	2			
T spine	2	2	2			
L spine	2	2	2			
Pelvis	2	2	2			
Upper Arms	2	2	2			
Lower Arms	0	0	0			
Femurs	2	2	2			
Lower Legs	0	0	0			
Soft tissue	0	0	0			
Total score	14	14	14			